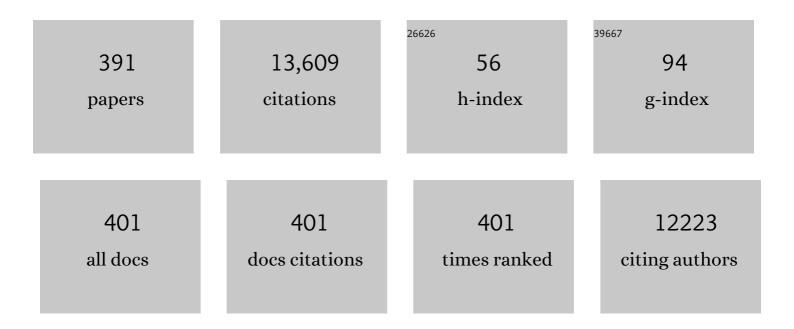
List of Publications by Year in descending order

Source: https://exaly.com/author-pdf/8792624/publications.pdf Version: 2024-02-01



#	Article	IF	CITATIONS
1	Impact of argon flow and pressure on the trapping behavior of nanoparticles inside a gas aggregation source. Plasma Processes and Polymers, 2022, 19, e2100125.	3.0	6
2	Sensing performance of CuO/Cu2O/ZnO:Fe heterostructure coated with thermally stable ultrathin hydrophobic PV3D3 polymer layer for battery application. Materials Today Chemistry, 2022, 23, 100642.	3.5	8
3	Adaptive Model for Magnetic Particle Mapping Using Magnetoelectric Sensors. Sensors, 2022, 22, 894.	3.8	1
4	In Situ Monitoring of Scale Effects on Phase Selection and Plasmonic Shifts during the Growth of AgCu Alloy Nanostructures for Anticounterfeiting Applications. ACS Applied Nano Materials, 2022, 5, 3832-3842.	5.0	7
5	Sparse CNT networks with implanted AgAu nanoparticles: A novel memristor with short-term memory bordering between diffusive and bipolar switching. PLoS ONE, 2022, 17, e0264846.	2.5	1
6	Selective Adsorption and Photocatalytic Cleanâ€Up of Oil by TiO ₂ Thin Film Decorated with pâ€V ₃ D ₃ Modified Flowerlike Ag Nanoplates. Advanced Materials Interfaces, 2022, 9, .	3.7	3
7	Brain-like critical dynamics and long-range temporal correlations in percolating networks of silver nanoparticles and functionality preservation after integration of insulating matrix. Nanoscale Advances, 2022, 4, 3149-3160.	4.6	11
8	Template-Induced Growth of Sputter-Deposited Gold Nanoparticles on Ordered Porous TiO ₂ Thin Films for Surface-Enhanced Raman Scattering Sensors. ACS Applied Nano Materials, 2022, 5, 7492-7501.	5.0	11
9	Selective Adsorption and Photocatalytic Cleanâ€Up of Oil by TiO ₂ Thin Film Decorated with pâ€V ₃ D ₃ Modified Flowerlike Ag Nanoplates (Adv. Mater. Interfaces 14/2022). Advanced Materials Interfaces, 2022, 9, .	3.7	0
10	Diffusion in metallic glasses and undercooled metallic melts. International Journal of Materials Research, 2022, 95, 956-960.	0.3	0
11	A thin-film broadband perfect absorber based on plasmonic copper nanoparticles. Micro and Nano Engineering, 2022, 16, 100154.	2.9	6
12	Tuning wettability of TiO2 thin film by photocatalytic deposition of 3D flower- and hedgehog-like Au nano- and microstructures. Applied Surface Science, 2021, 537, 147795.	6.1	16
13	Real-time insight into nanostructure evolution during the rapid formation of ultra-thin gold layers on polymers. Nanoscale Horizons, 2021, 6, 132-138.	8.0	24
14	Initiated Chemical Vapor Deposition (iCVD) Functionalized Polylactic Acid–Marine Algae Composite Patch for Bone Tissue Engineering. Polymers, 2021, 13, 186.	4.5	11
15	Enhancing Reliability of Studies on Single Filament Memristive Switching via an Unconventional cAFM Approach. Nanomaterials, 2021, 11, 265.	4.1	7
16	Revealing the growth of copper on polystyrene-block-poly(ethylene oxide) diblock copolymer thin films with in situ GISAXS. Nanoscale, 2021, 13, 10555-10565.	5.6	11
17	Synthesis and Investigation of a Photoswitchable Copolymer Deposited via Initiated Chemical Vapor Deposition for Application in Organic Smart Surfaces. ACS Applied Polymer Materials, 2021, 3, 1445-1456.	4.4	9
18	Molecular Insight into Real-Time Reaction Kinetics of Free Radical Polymerization from the Vapor Phase by In-Situ Mass Spectrometry. Journal of Physical Chemistry A, 2021, 125, 1661-1667.	2.5	9

#	Article	IF	CITATIONS
19	Exchange biased delta-E effect enables the detection of low frequency pT magnetic fields with simultaneous localization. Scientific Reports, 2021, 11, 5269.	3.3	27
20	Marine Algae Incorporated Polylactide Acid Patch: Novel Candidate for Targeting Osteosarcoma Cells without Impairing the Osteoblastic Proliferation. Polymers, 2021, 13, 847.	4.5	5
21	Influence of the piezoelectric material on the signal and noise of magnetoelectric magnetic field sensors based on the delta-E effect. APL Materials, 2021, 9, .	5.1	15
22	Magnetoelastic Coupling and Delta-E Effect in Magnetoelectric Torsion Mode Resonators. Sensors, 2021, 21, 2022.	3.8	16
23	Tailoring the Optical Properties of Sputter-Deposited Gold Nanostructures on Nanostructured Titanium Dioxide Templates Based on In Situ Grazing-Incidence Small-Angle X-ray Scattering Determined Growth Laws. ACS Applied Materials & Interfaces, 2021, 13, 14728-14740.	8.0	4
24	Improved Longâ€Term Stability and Reduced Humidity Effect in Gas Sensing: SiO ₂ Ultraâ€Thin Layered ZnO Columnar Films. Advanced Materials Technologies, 2021, 6, 2001137.	5.8	24
25	Selective Silver Nanocluster Metallization on Conjugated Diblock Copolymer Templates for Sensing and Photovoltaic Applications. ACS Applied Nano Materials, 2021, 4, 4245-4255.	5.0	14
26	Curvature and Stress Effects on the Performance of Contourâ€Mode Resonant Δ <i>E</i> Effect Magnetometers. Advanced Materials Technologies, 2021, 6, 2100294.	5.8	7
27	Epileptic Seizure Detection on an Ultra-Low-Power Embedded RISC-V Processor Using a Convolutional Neural Network. Biosensors, 2021, 11, 203.	4.7	19
28	TiO ₂ /Cu ₂ O/CuO Multi-Nanolayers as Sensors for H ₂ and Volatile Organic Compounds: An Experimental and Theoretical Investigation. ACS Applied Materials & Interfaces, 2021, 13, 32363-32380.	8.0	39
29	The sputter-based synthesis of tantalum oxynitride nanoparticles with architecture and bandgap controlled by design. Applied Surface Science, 2021, 559, 149974.	6.1	11
30	Heterostructure-based devices with enhanced humidity stability for H2 gas sensing applications in breath tests and portable batteries. Sensors and Actuators A: Physical, 2021, 329, 112804.	4.1	17
31	Tailoring the selectivity of ultralow-power heterojunction gas sensors by noble metal nanoparticle functionalization. Nano Energy, 2021, 88, 106241.	16.0	21
32	Enhancing composition control of alloy nanoparticles from gas aggregation source by in operando optical emission spectroscopy. Plasma Processes and Polymers, 2021, 18, 2000208.	3.0	12
33	Correlating Optical Reflectance with the Topology of Aluminum Nanocluster Layers Growing on Partially Conjugated Diblock Copolymer Templates. ACS Applied Materials & Interfaces, 2021, 13, 56663-56673.	8.0	9
34	Modeling and Parallel Operation of Exchange-Biased Delta-E Effect Magnetometers for Sensor Arrays. Sensors, 2021, 21, 7594.	3.8	3
35	Nucleation and Growth of Magnetronâ€6puttered Ag Nanoparticles as Witnessed by Timeâ€Resolved Small Angle Xâ€Ray Scattering. Particle and Particle Systems Characterization, 2020, 37, 1900436.	2.3	30
36	Facile fabrication of semiconducting oxide nanostructures by direct ink writing of readily available metal microparticles and their application as low power acetone gas sensors. Nano Energy, 2020, 70, 104420.	16.0	62

#	Article	IF	CITATIONS
37	Following in Situ the Deposition of Gold Electrodes on Low Band Gap Polymer Films. ACS Applied Materials & Interfaces, 2020, 12, 1132-1141.	8.0	10
38	Early osteoblastic activity on TiO ₂ thin films decorated with flower-like hierarchical Au structures. RSC Advances, 2020, 10, 28935-28940.	3.6	6
39	Fundamental Noise Limits and Sensitivity of Piezoelectrically Driven Magnetoelastic Cantilevers. Journal of Microelectromechanical Systems, 2020, 29, 1347-1361.	2.5	13
40	Single CuO/Cu ₂ O/Cu Microwire Covered by a Nanowire Network as a Gas Sensor for the Detection of Battery Hazards. ACS Applied Materials & Interfaces, 2020, 12, 42248-42263.	8.0	36
41	Mapping of magnetic nanoparticles and cells using thin film magnetoelectric sensors based on the delta-E effect. Sensors and Actuators A: Physical, 2020, 309, 112023.	4.1	9
42	Pd-Functionalized ZnO:Eu Columnar Films for Room-Temperature Hydrogen Gas Sensing: A Combined Experimental and Computational Approach. ACS Applied Materials & Interfaces, 2020, 12, 24951-24964.	8.0	34
43	Surface functionalization of ZnO:Ag columnar thin films with AgAu and AgPt bimetallic alloy nanoparticles as an efficient pathway for highly sensitive gas discrimination and early hazard detection in batteries. Journal of Materials Chemistry A, 2020, 8, 16246-16264.	10.3	38
44	Multi-Mode Love-Wave SAW Magnetic-Field Sensors. Sensors, 2020, 20, 3421.	3.8	18
45	Plasmonic and non-plasmonic contributions on photocatalytic activity of Au-TiO2 thin film under mixed UV–visible light. Surface and Coatings Technology, 2020, 389, 125613.	4.8	26
46	PdO nanoparticles decorated TiO2 film with enhanced photocatalytic and self-cleaning properties. Materials Today Chemistry, 2020, 16, 100251.	3.5	22
47	Nanoscale gradient copolymer films via single-step deposition from the vapor phase. Materials Today, 2020, 37, 35-42.	14.2	20
48	Fabrication of Diazocine-Based Photochromic Organic Thin Films via Initiated Chemical Vapor Deposition. Macromolecules, 2020, 53, 1164-1170.	4.8	12
49	Photodeposition of Au Nanoclusters for Enhanced Photocatalytic Dye Degradation over TiO ₂ Thin Film. ACS Applied Materials & Interfaces, 2020, 12, 14983-14992.	8.0	75
50	Marine Algae-PLA composites as de novo alternative to porcine derived collagen membranes. Materials Today Chemistry, 2020, 17, 100276.	3.5	16
51	Fabrication and Application of TEM-Compatible Sample Grids for Ex Situ Electrical Probing. IFMBE Proceedings, 2020, , 71-74.	0.3	1
52	Low-Temperature Solution Synthesis of Au-Modified ZnO Nanowires for Highly Efficient Hydrogen Nanosensors. ACS Applied Materials & Interfaces, 2019, 11, 32115-32126.	8.0	49
53	Antibacterial, highly hydrophobic and semi transparent Ag/plasma polymer nanocomposite coating on cotton fabric obtained by plasma based co-deposition. Cellulose, 2019, 26, 8877-8894.	4.9	34
54	Mechanical-Resonance-Enhanced Thin-Film Magnetoelectric Heterostructures for Magnetometers, Mechanical Antennas, Tunable RF Inductors, and Filters. Materials, 2019, 12, 2259.	2.9	53

#	Article	IF	CITATIONS
55	Correlating Nanostructure, Optical and Electronic Properties of Nanogranular Silver Layers during Polymer-Template-Assisted Sputter Deposition. ACS Applied Materials & Interfaces, 2019, 11, 29416-29426.	8.0	37
56	The evolution of Ag nanoparticles inside a gas aggregation cluster source. Plasma Processes and Polymers, 2019, 16, 1900079.	3.0	20
57	Tuning ZnO Sensors Reactivity toward Volatile Organic Compounds via Ag Doping and Nanoparticle Functionalization. ACS Applied Materials & Interfaces, 2019, 11, 31452-31466.	8.0	78
58	Frequency Dependency of the Delta-E Effect and the Sensitivity of Delta-E Effect Magnetic Field Sensors. Sensors, 2019, 19, 4769.	3.8	23
59	Wet-Chemical Assembly of 2D Nanomaterials into Lightweight, Microtube-Shaped, and Macroscopic 3D Networks. ACS Applied Materials & Interfaces, 2019, 11, 44652-44663.	8.0	30
60	Love Wave Magnetic Field Sensor Modeling $\hat{a} \in \hat{~}$ from 1D to 3D Model. , 2019, , .		1
61	Pathways to Tailor Photocatalytic Performance of TiO2 Thin Films Deposited by Reactive Magnetron Sputtering. Materials, 2019, 12, 2840.	2.9	59
62	Ag Nanoparticles Decorated TiO 2 Thin Films with Enhanced Photocatalytic Activity. Physica Status Solidi (A) Applications and Materials Science, 2019, 216, 1800898.	1.8	15
63	Superhydrophobic 3D Porous PTFE/TiO ₂ Hybrid Structures. Advanced Materials Interfaces, 2019, 6, 1801967.	3.7	19
64	3D-Printed Chemiresistive Sensor Array on Nanowire CuO/Cu ₂ O/Cu Heterojunction Nets. ACS Applied Materials & Interfaces, 2019, 11, 25508-25515.	8.0	52
65	Influence of the quality factor on the signal to noise ratio of magnetoelectric sensors based on the delta-E effect. Applied Physics Letters, 2019, 114, .	3.3	23
66	Evaporated electret films with superior charge stability based on Teflon AF 2400. Organic Electronics, 2019, 70, 167-171.	2.6	6
67	Effect of noble metal functionalization and film thickness on sensing properties of sprayed TiO2 ultra-thin films. Sensors and Actuators A: Physical, 2019, 293, 242-258.	4.1	19
68	Mutual interplay of ZnO micro- and nanowires and methylene blue during cyclic photocatalysis process. Journal of Environmental Chemical Engineering, 2019, 7, 103016.	6.7	92
69	Cauliflower-like CeO ₂ –TiO ₂ hybrid nanostructures with extreme photocatalytic and self-cleaning properties. Nanoscale, 2019, 11, 9840-9844.	5.6	24
70	Concept and modelling of memsensors as two terminal devices with enhanced capabilities in neuromorphic engineering. Scientific Reports, 2019, 9, 4361.	3.3	19
71	The impact of O ₂ /Ar ratio on morphology and functional properties in reactive sputtering of metal oxide thin films. Nanotechnology, 2019, 30, 235603.	2.6	20
72	Magnetic particle mapping using magnetoelectric sensors as an imaging modality. Scientific Reports, 2019, 9, 2086.	3.3	23

#	Article	IF	CITATIONS
73	Superhydrophobic Surfaces: Superhydrophobic 3D Porous PTFE/TiO2 Hybrid Structures (Adv. Mater.) Tj ETQq1 1	0.784314	rgBT /Over
74	Tunable polytetrafluoroethylene electret films with extraordinary charge stability synthesized by initiated chemical vapor deposition for organic electronics applications. Scientific Reports, 2019, 9, 2237.	3.3	28
75	Diffusive Memristive Switching on the Nanoscale, from Individual Nanoparticles towards Scalable Nanocomposite Devices. Scientific Reports, 2019, 9, 17367.	3.3	23
76	Magnetic Sensitivity of Bending-Mode Delta-E-Effect Sensors. Physical Review Applied, 2019, 12, .	3.8	18
77	PTFEP–Al ₂ O ₃ hybrid nanowires reducing thrombosis and biofouling. Nanoscale Advances, 2019, 1, 4659-4664.	4.6	10
78	Nanogenerator and piezotronic inspired concepts for energy efficient magnetic field sensors. Nano Energy, 2019, 56, 420-425.	16.0	14
79	Electret films with extremely high charge stability prepared by thermal evaporation of Teflon AF. Organic Electronics, 2018, 57, 146-150.	2.6	21
80	A comparative study of photocatalysis on highly active columnar TiO2 nanostructures in-air and in-solution. Solar Energy Materials and Solar Cells, 2018, 178, 170-178.	6.2	59
81	Wide Band Low Noise Love Wave Magnetic Field Sensor System. Scientific Reports, 2018, 8, 278.	3.3	89
82	(CuO-Cu2O)/ZnO:Al heterojunctions for volatile organic compound detection. Sensors and Actuators B: Chemical, 2018, 255, 1362-1375.	7.8	47
83	Self-organized nanocrack networks: a pathway to enlarge catalytic surface area in sputtered ceramic thin films, showcased for photocatalytic TiO ₂ . Nanotechnology, 2018, 29, 035703.	2.6	20
84	Tuning doping and surface functionalization of columnar oxide films for volatile organic compound sensing: experiments and theory. Journal of Materials Chemistry A, 2018, 6, 23669-23682.	10.3	36
85	Magnetron-sputtered copper nanoparticles: lost in gas aggregation and found by <i>in situ</i> X-ray scattering. Nanoscale, 2018, 10, 18275-18281.	5.6	46
86	Nanoparticle forming reactive plasmas: a multidiagnostic approach. European Physical Journal D, 2018, 72, 1.	1.3	6
87	Plasma based formation and deposition of metal and metal oxide nanoparticles using a gas aggregation source. European Physical Journal D, 2018, 72, 1.	1.3	29
88	Photocatalytic Growth of Hierarchical Au Needle Clusters on Highly Active TiO ₂ Thin Film. Advanced Materials Interfaces, 2018, 5, 1800465.	3.7	21
89	PdO/PdO ₂ functionalized ZnO : Pd films for lower operating temperature H ₂ gas sensing. Nanoscale, 2018, 10, 14107-14127.	5.6	114
90	Role of UV Plasmonics in the Photocatalytic Performance of TiO ₂ Decorated with Aluminum Nanoparticles. ACS Applied Nano Materials, 2018, 1, 3760-3764.	5.0	35

#	Article	IF	CITATIONS
91	Ultra-thin TiO2 films by atomic layer deposition and surface functionalization with Au nanodots for sensing applications. Materials Science in Semiconductor Processing, 2018, 87, 44-53.	4.0	30
92	Hierarchical Structures: Photocatalytic Growth of Hierarchical Au Needle Clusters on Highly Active TiO ₂ Thin Film (Adv. Mater. Interfaces 15/2018). Advanced Materials Interfaces, 2018, 5, 1870074.	3.7	1
93	Formation of polymer-based nanoparticles and nanocomposites by plasma-assisted deposition methods. European Physical Journal D, 2018, 72, 1.	1.3	8
94	Role of Sputter Deposition Rate in Tailoring Nanogranular Gold Structures on Polymer Surfaces. ACS Applied Materials & Interfaces, 2017, 9, 5629-5637.	8.0	64
95	Atomic dynamics in Zr-based glass forming alloys near the liquidus temperature. Physical Review B, 2017, 95, .	3.2	20
96	Localized Synthesis of Iron Oxide Nanowires and Fabrication of High Performance Nanosensors Based on a Single Fe ₂ O ₃ Nanowire. Small, 2017, 13, 1602868.	10.0	111
97	Single target sputter deposition of alloy nanoparticles with adjustable composition via a gas aggregation cluster source. Nanotechnology, 2017, 28, 175703.	2.6	52
98	Tuning silver ion release properties in reactively sputtered Ag/TiOx nanocomposites. Applied Physics A: Materials Science and Processing, 2017, 123, 1.	2.3	7
99	Modeling and Analysis of Noise Sources for Thin-Film Magnetoelectric Sensors Based on the Delta-E Effect. IEEE Transactions on Instrumentation and Measurement, 2017, 66, 2771-2779.	4.7	24
100	Ultra-fast degradation of methylene blue by Au/ZnO-CeO2 nano-hybrid catalyst. Materials Letters, 2017, 209, 486-491.	2.6	20
101	Extreme tuning of wetting on 1D nanostructures: from a superhydrophilic to a perfect hydrophobic surface. Nanoscale, 2017, 9, 14814-14819.	5.6	12
102	Light-induced Conductance Switching in Photomechanically Active Carbon Nanotube-Polymer Composites. Scientific Reports, 2017, 7, 9648.	3.3	11
103	Single-step generation of metal-plasma polymer multicore@shell nanoparticles from the gas phase. Scientific Reports, 2017, 7, 8514.	3.3	27
104	Modification of a metal nanoparticle beam by a hollow electrode discharge. Journal of Vacuum Science and Technology A: Vacuum, Surfaces and Films, 2016, 34, 021301.	2.1	2
105	Molecular dynamics simulation of gold cluster growth during sputter deposition. Journal of Applied Physics, 2016, 119, .	2.5	28
106	Controlled synthesis of germanium nanoparticles by nonthermal plasmas. Applied Physics Letters, 2016, 108, .	3.3	12
107	Influence of nanoparticle formation on discharge properties in argon-acetylene capacitively coupled radio frequency plasmas. Applied Physics Letters, 2016, 108, .	3.3	20
108	Multimode delta-E effect magnetic field sensors with adapted electrodes. Applied Physics Letters, 2016, 108, .	3.3	48

#	Article	IF	CITATIONS
109	Non-planar nanoscale p–p heterojunctions formation in Zn Cu1O nanocrystals by mixed phases for enhanced sensors. Sensors and Actuators B: Chemical, 2016, 230, 832-843.	7.8	70
110	Adaptive Readout Schemes for Thin-Film Magnetoelectric Sensors Based on the delta-E Effect. IEEE Sensors Journal, 2016, 16, 4891-4900.	4.7	26
111	Multifunctional device based on ZnO:Fe nanostructured films with enhanced UV and ultra-fast ethanol vapour sensing. Materials Science in Semiconductor Processing, 2016, 49, 20-33.	4.0	73
112	Enhanced ethanol vapour sensing performances of copper oxide nanocrystals with mixed phases. Sensors and Actuators B: Chemical, 2016, 224, 434-448.	7.8	140
113	Photocatalytic properties of titania thin films prepared by sputtering versus evaporation and aging of induced oxygen vacancy defects. Applied Catalysis B: Environmental, 2016, 180, 362-371.	20.2	54
114	Characterization of a radio frequency hollow electrode discharge at low gas pressures. Physics of Plasmas, 2015, 22, .	1.9	11
115	Phase modulated magnetoelectric delta-E effect sensor for sub-nano tesla magnetic fields. Applied Physics Letters, 2015, 107, .	3.3	74
116	Adaptive Multi-mode Combination for Magnetoelectric Sensors Based on the Delta-E Effect. Procedia Engineering, 2015, 120, 536-539.	1.2	5
117	Real-Time Monitoring of Morphology and Optical Properties during Sputter Deposition for Tailoring Metal–Polymer Interfaces. ACS Applied Materials & Interfaces, 2015, 7, 13547-13556.	8.0	113
118	X-ray spectroscopy characterization of azobenzene-functionalized triazatriangulenium adlayers on Au(111) surfaces. Physical Chemistry Chemical Physics, 2015, 17, 17053-17062.	2.8	26
119	Stable production of TiO _x nanoparticles with narrow size distribution by reactive pulsed dc magnetron sputtering. Journal Physics D: Applied Physics, 2015, 48, 035501.	2.8	24
120	Simulation of nanocolumn formation in a plasma environment. Journal of Applied Physics, 2015, 117, 014305.	2.5	7
121	Free Volume Profiles at Polymer–Solid Interfaces Probed by Focused Slow Positron Beam. Macromolecules, 2015, 48, 1493-1498.	4.8	9
122	Versatile particle collection concept for correlation of particle growth and discharge parameters in dusty plasmas. Journal Physics D: Applied Physics, 2015, 48, 055203.	2.8	15
123	Free Volume and Gas Permeation in Anthracene Maleimide-Based Polymers of Intrinsic Microporosity. Membranes, 2015, 5, 214-227.	3.0	18
124	Light-Controlled Conductance Switching in Azobenzene-Containing MWCNT–Polymer Nanocomposites. ACS Applied Materials & Interfaces, 2015, 7, 11257-11262.	8.0	38
125	Quantitative Evaluation of Contamination on Dental Zirconia Ceramic by Silicone Disclosing Agents after Different Cleaning Procedures. Materials, 2015, 8, 2650-2657.	2.9	7
126	Light-induced conductance switching in azobenzene based near-percolated single wall carbon nanotube/polymer composites. Carbon, 2015, 90, 94-101.	10.3	22

#	Article	IF	CITATIONS
127	The effect of low-temperature structural relaxation on free volume and chemical short-range ordering in a Au49Cu26.9Si16.3Ag5.5Pd2.3 bulk metallic glass. Scripta Materialia, 2015, 103, 14-17.	5.2	40
128	Light-Triggered Control of Plasmonic Refraction and Group Delay by Photochromic Molecular Switches. ACS Photonics, 2015, 2, 1327-1332.	6.6	20
129	Correlation of gas permeation and free volume in new and used high free volume thin film composite membranes. Journal of Polymer Science, Part B: Polymer Physics, 2015, 53, 213-217.	2.1	25
130	Microstructural and plasmonic modifications in Ag–TiO ₂ and Au–TiO ₂ nanocomposites through ion beam irradiation. Beilstein Journal of Nanotechnology, 2014, 5, 1419-1431.	2.8	40
131	Effective Optical Properties of Plasmonic Nanocomposites. Materials, 2014, 7, 727-741.	2.9	50
132	Interphases in Polymer Solid-Contacts and Nanocomposites Probed by Positron Annihilation Lifetime Spectroscopy. Soft Materials, 2014, 12, S135-S141.	1.7	8
133	Review of Plasmonic Nanocomposite Metamaterial Absorber. Materials, 2014, 7, 1221-1248.	2.9	149
134	High-Voltage Insulation Organic-Inorganic Nanocomposites by Plasma Polymerization. Materials, 2014, 7, 563-575.	2.9	18
135	Decoupling of Component Diffusion in a Glass-Forming <mml:math xmlns:mml="http://www.w3.org/1998/Math/MathML" display="inline"><mml:mrow><mml:msub><mml:mrow><mml:mi>Zr</mml:mi></mml:mrow><mml:mrow><mm Physical Review Letters, 2014, 113, 165901.</mm </mml:mrow></mml:msub></mml:mrow></mml:math 	nl:m71846.7	5< 7 mml:mro
136	Plasmonic tunable metamaterial absorber as ultraviolet protection film. Applied Physics Letters, 2014, 104, .	3.3	95
137	Giant magnetoelectric effect at low frequencies in polymer-based thin film composites. Applied Physics Letters, 2014, 104, .	3.3	48
138	Photoâ€driven Super Absorber as an Active Metamaterial with a Tunable Molecularâ€Plasmonic Coupling. Advanced Optical Materials, 2014, 2, 705-710.	7.3	38
139	Controlling surface segregation of reactively sputtered Ag/TiOx nanocomposites. Acta Materialia, 2014, 74, 1-8.	7.9	14
140	Microelectromechanical magnetic field sensor based on Δ <i>E</i> effect. Applied Physics Letters, 2014, 105, .	3.3	59
141	Spectroelectrochemical and morphological studies of the ageing of silver nanoparticles embedded in ultra-thin perfluorinated sputter deposited films. Thin Solid Films, 2014, 571, 161-167.	1.8	0
142	Interphase of a Polymer at a Solid Interface. Macromolecules, 2014, 47, 8459-8465.	4.8	22
143	Metamaterials: Photo-driven Super Absorber as an Active Metamaterial with a Tunable Molecular-Plasmonic Coupling (Advanced Optical Materials 8/2014). Advanced Optical Materials, 2014, 2, 704-704.	7.3	2
144	The hybrid concept for realization of an ultra-thin plasmonic metamaterial antireflection coating and plasmonic rainbow. Nanoscale, 2014, 6, 6037-6045.	5.6	52

#	Article	IF	CITATIONS
145	Free volume in PEP-silica nanocomposites with varying molecular weight. Polymer, 2014, 55, 143-149.	3.8	9
146	Kinetic Monte Carlo Simulations of Cluster Growth and Diffusion in Metal-Polymer Nanocomposites. Springer Series on Atomic, Optical, and Plasma Physics, 2014, , 321-370.	0.2	4
147	Effect of gold alloying on stability of silver nanoparticles and control of silver ion release from vapor-deposited Ag–Au/polytetrafluoroethylene nanocomposites. Gold Bulletin, 2013, 46, 3-11.	2.4	48
148	High rate deposition system for metal-cluster/SiO x C y H z –polymer nanocomposite thin films. Journal of Nanoparticle Research, 2013, 15, 1.	1.9	21
149	Huge increase in gas phase nanoparticle generation by pulsed direct current sputtering in a reactive gas admixture. Applied Physics Letters, 2013, 103, .	3.3	35
150	Huge increase of therapeutic window at a bioactive silver/titania nanocomposite coating surface compared to solution. Materials Science and Engineering C, 2013, 33, 2367-2375.	7.3	14
151	Plasma-polymerized HMDSO coatings to adjust the silver ion release properties of Ag/polymer nanocomposites. Journal of Nanoparticle Research, 2013, 15, 1.	1.9	32
152	Role of oxygen admixture in stabilizing TiO x nanoparticle deposition from a gas aggregation source. Journal of Nanoparticle Research, 2013, 15, 1.	1.9	21
153	Formation of magnetic nanocolumns during vapor phase deposition of a metal-polymer nanocomposite: Experiments and kinetic Monte Carlo simulations. Journal of Applied Physics, 2013, 114,	2.5	16
154	Vapour phase deposition of highly crystalline self-poled piezoelectric nylon-11. Journal Physics D: Applied Physics, 2012, 45, 055304.	2.8	15
155	Preparation of Silver Nanoparticles-Nafion Membrane Composite by Photoreduction Process. ECS Transactions, 2012, 41, 9-18.	0.5	3
156	Surface segregation in TiO ₂ -based nanocomposite thin films. Nanotechnology, 2012, 23, 495701.	2.6	27
157	Influence of reactive gas admixture on transition metal cluster nucleation in a gas aggregation cluster source. Journal of Applied Physics, 2012, 112, .	2.5	44
158	Tunable broadband plasmonic perfect absorber at visible frequency. Applied Physics A: Materials Science and Processing, 2012, 109, 769-773.	2.3	80
159	Aging and Free Volume in a Polymer of Intrinsic Microporosity (PIM-1). Journal of Adhesion, 2012, 88, 608-619.	3.0	79
160	A critical evaluation of the 0–3 approach for magnetoelectric nanocomposites with metallic nanoparticles. Journal of Applied Physics, 2012, 112, 044303.	2.5	9
161	Towards a Particle Based Simulation of Complex Plasma Driven Nanocomposite Formation. Contributions To Plasma Physics, 2012, 52, 890-898.	1.1	20
162	Mass Spectrometric Investigations of Nano‣ize Cluster Ions Produced by High Pressure Magnetron Sputtering. Contributions To Plasma Physics, 2012, 52, 881-889.	1.1	40

#	Article	IF	CITATIONS
163	Monitoring magnetostriction by a quantum tunnelling strain sensor. Sensors and Actuators A: Physical, 2012, 183, 28-33.	4.1	3
164	Simple method of hybrid PVD/PECVD to prepare well-dispersed cobalt–plasma polymerized hexamethyldisilazane nanocomposites. Surface and Coatings Technology, 2012, 207, 565-570.	4.8	5
165	Highly versatile concept for precise tailoring of nanogranular composites with a gas aggregation cluster source. Applied Physics Letters, 2012, 100, .	3.3	11
166	Tuning of the ion release properties of silver nanoparticles buried under a hydrophobic polymer barrier. Journal of Nanoparticle Research, 2012, 14, 1.	1.9	46
167	Vapor Phase Deposition, Structure, and Plasmonic Properties of Polymer-Based Composites Containing Ag–Cu Bimetallic Nanoparticles. Plasmonics, 2012, 7, 107-114.	3.4	21
168	Advances in top–down and bottom–up surface nanofabrication: Techniques, applications & future prospects. Advances in Colloid and Interface Science, 2012, 170, 2-27.	14.7	659
169	Combined in situ electrochemical impedance spectroscopy–UV/Vis and AFM studies of Ag nanoparticle stability in perfluorinated films. Materials Chemistry and Physics, 2012, 134, 302-308.	4.0	6
170	Fully integrable magnetic field sensor based on delta-E effect. Applied Physics Letters, 2011, 99, 223502.	3.3	82
171	Diffusion and viscous flow in bulk glass forming alloys. Journal of Alloys and Compounds, 2011, 509, S2-S7.	5.5	6
172	Metal/polymer nanocomposite thin films prepared by plasma polymerization and high pressure magnetron sputtering. Surface and Coatings Technology, 2011, 205, S38-S41.	4.8	25
173	The method of conventional calorimetric probes — A short review and application for the characterization of nanocluster sources. Surface and Coatings Technology, 2011, 205, S388-S392.	4.8	20
174	Study of cobalt clusters with very narrow size distribution deposited by high-rate cluster source. Nanotechnology, 2011, 22, 465704.	2.6	23
175	Fast electrical response to volatile organic compounds of 2D Au nanoparticle layers embedded into polymers. Journal of Materials Science, 2011, 46, 438-445.	3.7	16
176	Optical switching behavior of azobenzene/PMMA blends with high chromophore concentration. Journal of Materials Science, 2011, 46, 2488-2494.	3.7	18
177	Morphological and magnetic properties of TiO2/Fe50Co50 composite films. Journal of Materials Science, 2011, 46, 4638-4645.	3.7	6
178	Reversible light-induced capacitance switching of azobenzene ether/PMMA blends. Applied Physics A: Materials Science and Processing, 2011, 102, 421-427.	2.3	10
179	Free volume changes on optical switching in azobenzeneâ€polymethylmethacrylate blends studied by a pulsed lowâ€energy positron beam. Journal of Polymer Science, Part B: Polymer Physics, 2011, 49, 404-408.	2.1	8
180	An Omnidirectional Transparent Conductingâ€Metalâ€Based Plasmonic Nanocomposite. Advanced Materials, 2011, 23, 1993-1997.	21.0	44

#	Article	IF	CITATIONS
181	Design of a Perfect Black Absorber at Visible Frequencies Using Plasmonic Metamaterials. Advanced Materials, 2011, 23, 5410-5414.	21.0	425
182	Perfect Plasmonic Absorber: Design of a Perfect Black Absorber at Visible Frequencies Using Plasmonic Metamaterials (Adv. Mater. 45/2011). Advanced Materials, 2011, 23, 5409-5409.	21.0	1
183	Diffusion and Growth of Metal Clusters in Nanocomposites: A Kinetic Monte Carlo Study. Contributions To Plasma Physics, 2011, 51, 971-980.	1.1	13
184	In situ atomic force microscopy studies of reversible light-induced switching of surface roughness and adhesion in azobenzene-containing PMMA films. Applied Surface Science, 2011, 257, 7719-7726.	6.1	7
185	Free volume distribution at the Teflon AF®/silicon interfaces probed by a slow positron beam. Polymer, 2011, 52, 505-509.	3.8	11
186	Nanostructural and Functional Properties of Ag-TiO ₂ Coatings Prepared by Co-Sputtering Deposition Technique. Journal of Nanoscience and Nanotechnology, 2011, 11, 4893-4899.	0.9	14
187	Reactive epoxies with functional zeolite fillers: IR spectroscopy and PALS studies. Journal of Materials Research, 2011, 26, 2877-2886.	2.6	3
188	Modification of polyethylene powder with an organic precursor in a spiral conveyor by hollow cathode glow discharge. European Physical Journal D, 2010, 58, 305-310.	1.3	19
189	Preparation and plasmonic properties of polymer-based composites containing Ag–Au alloy nanoparticles produced by vapor phase co-deposition. Journal of Materials Science, 2010, 45, 5865-5871.	3.7	47
190	Subnanometre size free volumes in amorphous Verapamil hydrochloride: A positron lifetime and PVT study through Tg in comparison with dielectric relaxation spectroscopy. European Journal of Pharmaceutical Sciences, 2010, 41, 388-398.	4.0	8
191	Metalâ€Polymer Nanocomposites for Functional Applications. Advanced Engineering Materials, 2010, 12, 1177-1190.	3.5	209
192	Free Volume and Swelling in Thin Films of Poly(<i>N</i> â€isopropylacrylamide) Endâ€Capped with <i>n</i> â€Butyltrithiocarbonate. Macromolecular Rapid Communications, 2010, 31, 1364-1367.	3.9	21
193	Molecular dynamics approach to structure–property correlation in epoxy resins for thermo-mechanical lifetime modeling. Microelectronics Reliability, 2010, 50, 900-909.	1.7	23
194	Shelf stability of reactive adhesive formulations: A case study for dicyandiamide-cured epoxy systems. International Journal of Adhesion and Adhesives, 2010, 30, 105-110.	2.9	35
195	Residual stress in polytetrafluoroethylene-metal nanocomposite films prepared by magnetron sputtering. Thin Solid Films, 2010, 518, 5944-5949.	1.8	16
196	Free volume from positron lifetime and pressure–volume–temperature experiments in relation to structural relaxation of van der Waals molecular glass-forming liquids. Journal of Physics Condensed Matter, 2010, 22, 235104.	1.8	13
197	Synthesis and Characterization of Ag-Polymer Nanocomposites. Journal of Nanoscience and Nanotechnology, 2010, 10, 2833-2837.	0.9	47
198	Reversible light-controlled conductance switching of azobenzene-based metal/polymer nanocomposites. Nanotechnology, 2010, 21, 465201.	2.6	27

#	Article	IF	CITATIONS
199	Free Volume Investigation of Polymers of Intrinsic Microporosity (PIMs): PIM-1 and PIM1 Copolymers Incorporating Ethanoanthracene Units. Macromolecules, 2010, 43, 6075-6084.	4.8	100
200	Free Volume of Interphases in Model Nanocomposites Studied by Positron Annihilation Lifetime Spectroscopy. Macromolecules, 2010, 43, 10505-10511.	4.8	51
201	Dynamic Arrest in Multicomponent Glass-Forming Alloys. Physical Review Letters, 2010, 104, 195901.	7.8	103
202	Formation of TiO-single crystals in Ag-TiO2 based nanocomposites by swift heavy ion irradiation. , 2009, , .		0
203	Molecular dynamics approach to structure-property correlation in epoxy resins for thermo-mechanical lifetime modeling. , 2009, , .		11
204	The temperature dependence of free volume in phenyl salicylate and its relation to structural dynamics: A positron annihilation lifetime and pressure-volume-temperature study. Journal of Chemical Physics, 2009, 130, 144906.	3.0	18
205	Fabrication of Toroidal Microinductors for RF Applications. IEEE Transactions on Magnetics, 2009, 45, 4770-4772.	2.1	7
206	Structural characteristics of a multilayer of silicon rich oxide (SRO) with high Si content prepared by LPCVD. Physica Status Solidi (A) Applications and Materials Science, 2009, 206, 263-269.	1.8	10
207	Gas permeability and free volume in poly(amide-b-ethylene oxide)/polyethylene glycol blend membranes. Journal of Membrane Science, 2009, 339, 177-183.	8.2	124
208	Molecular dynamics simulation and mechanical characterisation for the establishment of structure-property correlations for epoxy resins in microelectronics packaging applications. , 2009, , .		9
209	Controlled reduction of size of Ag nanoparticles embedded in teflon matrix by MeV ion irradiation. Nuclear Instruments & Methods in Physics Research B, 2008, 266, 1804-1809.	1.4	34
210	XPS study of the initial oxidation of the bulk metallic glass Zr46.75Ti8.25Cu7.5Ni10Be27.5. Journal of Materials Science, 2008, 43, 5495-5503.	3.7	23
211	Tuning of electrical and structural properties of metal-polymer nanocomposite films prepared by co-evaporation technique. Applied Physics A: Materials Science and Processing, 2008, 92, 345-350.	2.3	57
212	Positron annihilation lifetime measurements of mechanically fatigued polystyrene samples. Journal of Polymer Science, Part B: Polymer Physics, 2008, 46, 1991-1995.	2.1	4
213	Influence of top layer geometries on the electronic properties of pentacene and diindenoperylene thin films. Physica Status Solidi (A) Applications and Materials Science, 2008, 205, 578-590.	1.8	14
214	An ion track based approach to nano- and micro-electronics. Nuclear Instruments & Methods in Physics Research B, 2008, 266, 1642-1646.	1.4	38
215	Polymer-metal nanocomposites with 2-dimensional Au nanoparticle arrays for sensoric applications. Journal of Physics: Conference Series, 2008, 100, 052043.	0.4	21
216	Temperature Dependence of the Free Volume in Amorphous Teflon AF1600 and AF2400: A Pressureâ^'Volumeâ^'Temperature and Positron Lifetime Study. Macromolecules, 2008, 41, 6125-6133.	4.8	53

#	Article	IF	CITATIONS
217	Temperature Dependence of Positron Annihilation Lifetimes in High Permeability Polymers:  Amorphous Teflons AF. Macromolecules, 2008, 41, 788-795.	4.8	49
218	Plasmonic properties of vapour-deposited polymer composites containing Ag nanoparticles and their changes upon annealing. Journal Physics D: Applied Physics, 2008, 41, 125409.	2.8	23
219	Equal intensity double plasmon resonance of bimetallic quasi-nanocomposites based on sandwich geometry. Nanotechnology, 2008, 19, 225302.	2.6	28
220	Temperature dependence of the free volume from positron lifetime experiments and its relation to structural dynamics: Phenylphthalein-dimethylether. Physical Review E, 2008, 78, 051505.	2.1	14
221	Functional Polymer Nanocomposites. Polymers and Polymer Composites, 2008, 16, 471-481.	1.9	48
222	Tuning the threshold voltage of organic field-effect transistors by an electret encapsulating layer. Applied Physics Letters, 2007, 90, 013501.	3.3	36
223	Diffusion in Bulk Glass Forming Alloys– from the Glass to the Equilibrium Melt. Defect and Diffusion Forum, 2007, 266, 109-118.	0.4	0
224	Boltorn-Modified Poly(2,6-dimethyl-1,4-phenylene oxide) Gas Separation Membranes. Macromolecules, 2007, 40, 5400-5410.	4.8	41
225	Diffusion in bulk-metallic glass-forming Pd–Cu–Ni–P alloys: From the glass to the equilibrium melt. Journal of Non-Crystalline Solids, 2007, 353, 3285-3289.	3.1	22
226	Toroid microinductors with magnetic nanocomposite cores. , 2007, , .		2
227	Improved effective medium approach: Application to metal nanocomposites. Journal of Applied Physics, 2007, 101, 024302.	2.5	20
228	Model Systems with Extreme Aspect Ratio, Tunable Geometry, and Surface Functionality for a Quantitative Investigation of the Lotus Effect. Langmuir, 2007, 23, 2091-2094.	3.5	29
229	Free Volume in C ₆₀ Modified PPO Polymer Membranes by Positron Annihilation Lifetime Spectroscopy. Journal of Physical Chemistry B, 2007, 111, 13914-13918.	2.6	26
230	Deposition of Nanocomposites by Plasmas. Contributions To Plasma Physics, 2007, 47, 537-544.	1.1	53
231	Characterization of Au nano-cluster formation on and diffusion in polystyrene using XPS peak shape analysis. Surface Science, 2007, 601, 3261-3267.	1.9	50
232	Investigations into Composition and Structure of DBD-Deposited Amino Group Containing Polymer Layers. Plasma Processes and Polymers, 2007, 4, S482-486.	3.0	28
233	Unusual temperature dependence of the positron lifetime in a polymer of intrinsic microporosity. Physica Status Solidi - Rapid Research Letters, 2007, 1, 190-192.	2.4	32
234	Surface glass transition in bimodal polystyrene mixtures. European Physical Journal E, 2007, 24, 243-246.	1.6	9

#	Article	IF	CITATIONS
235	Study of air oxidation of amorphous Zr65Cu17.5Ni10Al7.5 by X-ray photoelectron spectroscopy (XPS). Journal of Materials Science, 2007, 42, 9037-9044.	3.7	11
236	Effects of ion beam treatment on atomic and macroscopic adhesion of copper to different polymer materials. Nuclear Instruments & Methods in Physics Research B, 2007, 265, 139-145.	1.4	25
237	Study of air oxidation of amorphous Zr65Cu17.5Ni10Al7.5 by X-ray photoelectron spectroscopy (XPS). , 2007, 42, 9037.		1
238	Depth-Resolved Analysis of the Aging Behavior of Epoxy Thin Films by Positron Spectroscopy. , 2006, , 465-477.		2
239	Self-organization of ultrahigh-density Fe–Ni–Co nanocolumns in Teflon® AF. Applied Physics Letters, 2006, 88, 123103.	3.3	18
240	Plasmonic properties of Ag nanoclusters in various polymer matrices. Nanotechnology, 2006, 17, 3499-3505.	2.6	138
241	Controlled growth of Au nanoparticles in co-evaporated metal/polymer composite films and their optical and electrical properties. EPJ Applied Physics, 2006, 33, 83-89.	0.7	39
242	Nanostructured magnetic Fe–Ni–Co/Teflon multilayers for high-frequency applications in the gigahertz range. Applied Physics Letters, 2006, 89, 242501.	3.3	71
243	Vapor-induced crystallization behavior of bisphenol-A polycarbonate. Polymer Engineering and Science, 2006, 46, 729-734.	3.1	37
244	Optical and electrical properties of polymer metal nanocomposites prepared by magnetron co-sputtering. Thin Solid Films, 2006, 515, 801-804.	1.8	85
245	Dispersion of gold nanoclusters in TMBPA-polycarbonate by a combination of thermal embedding and vapour-induced crystallization. Journal Physics D: Applied Physics, 2006, 39, 5086-5090.	2.8	5
246	Physico-chemical and antimicrobial properties of co-sputtered Ag–Au/PTFE nanocomposite coatings. Nanotechnology, 2006, 17, 4904-4908.	2.6	124
247	Codiffusion of P32 and Co57 in glass-forming Pd43Cu27Ni10P20 alloy and its relation to viscosity. Applied Physics Letters, 2006, 89, 121917.	3.3	18
248	Radiotracer Diffusion Measurements of Noble Metal Atoms in Semiconducting Organic Films Materials Research Society Symposia Proceedings, 2005, 871, 1.	0.1	2
249	Ag-Diffusion in the Organic Semiconductor Diindenoperylene. Defect and Diffusion Forum, 2005, 237-240, 993-997.	0.4	7
250	Molecular dynamics simulations of interactions of Ar and Xe ions with surface Cu clusters at low impact energies. Nuclear Instruments & Methods in Physics Research B, 2005, 228, 41-45.	1.4	9
251	Molecular dynamics simulations of low energy ion sputtering of copper nano-dimensional clusters on graphite substrates. Nuclear Instruments & Methods in Physics Research B, 2005, 227, 261-270.	1.4	21
252	Tailoring of the PS surface with low energy ions: Relevance to growth and adhesion of noble metals. Nuclear Instruments & Methods in Physics Research B, 2005, 236, 95-102.	1.4	38

#	Article	lF	CITATIONS
253	Investigation of the drastic change in the sputter rate of polymers at low ion fluence. Nuclear Instruments & Methods in Physics Research B, 2005, 236, 241-248.	1.4	46
254	Formation of a metal/epoxy resin interface. Applied Surface Science, 2005, 239, 227-236.	6.1	30
255	Molecular Dynamics Simulation of the Interaction of Low-Energy Ar and Xe lons with Copper Clusters on a Graphite Surface. Physics of the Solid State, 2005, 47, 1986.	0.6	Ο
256	(La0.8,Sr0.2)MnO3â^•Ti-metal foil substrate heterostructure effects on the ferroelectric and piezoelectric properties of lead zirconate titanate thin films. Applied Physics Letters, 2005, 87, 182910.	3.3	3
257	Radiotracer measurements as a sensitive tool for the detection of metal penetration in molecular-based organic electronics. Applied Physics Letters, 2005, 86, 024104.	3.3	33
258	Size evolution effect of the reduction rate on the synthesis of gold nanoparticles. Advanced Powder Technology, 2005, 16, 137-144.	4.1	8
259	Diffusion in Metallic Glasses and Supercooled Melts. , 2005, , 249-282.		4
260	Metal Diffusion in Polymers and on Polymer Surfaces. , 2005, , 333-363.		5
261	Controlled syntheses of Ag–polytetrafluoroethylene nanocomposite thin films by co-sputtering from two magnetron sources. Nanotechnology, 2005, 16, 1078-1082.	2.6	122
262	Metal Diffusion in Polymers and on Polymer Surfaces. , 2005, , 333-363.		9
263	Free Volume in Polyimides:Â Positron Annihilation Experiments and Molecular Modeling. Macromolecules, 2005, 38, 9638-9643.	4.8	82
264	Arrays of wirelike microstructures of Ag with visible wavelength transparent plasmonic response at near-ultraviolet and midinfrared regions. Applied Physics Letters, 2004, 85, 1952-1954.	3.3	2
265	Positron Annihilation Spectroscopy in Polymers. Materials Science Forum, 2004, 445-446, 219-223.	0.3	22
266	In Situ Investigations on the Cross-Linking Process of the Epoxy Resin System DGEBA-DETA by Means of Positron Annihilation Lifetime Spectroscopy in Comparison with Infrared Spectroscopy. Materials Science Forum, 2004, 445-446, 313-315.	0.3	4
267	Strain-controlled growth of nanowires within thin-film cracks. Nature Materials, 2004, 3, 375-379.	27.5	140
268	Nanoparticle architecture in carbonaceous matrix upon swift heavy ion irradiation of polymer–metal nanocomposites. Nuclear Instruments & Methods in Physics Research B, 2004, 217, 39-50.	1.4	25
269	Etched ion tracks in silicon oxide and silicon oxynitride as charge injection or extraction channels for novel electronic structures. Nuclear Instruments & Methods in Physics Research B, 2004, 218, 355-361.	1.4	61
270	Effects of thermal annealing of thin Au film on Fe40Ni38Mo4B18in ultrahigh vacuum (UHV). Journal of Materials Science, 2004, 39, 6291-6297.	3.7	6

#	Article	IF	CITATIONS
271	Free volume changes in mechanically milled PS and PC studied by positron annihilation lifetime spectroscopy (PALS). Polymer Engineering and Science, 2004, 44, 1351-1359.	3.1	9
272	Quenching rate dependence of free volume in a Zr-Cu-Ni-Ti-Be glass as probed by positron annihilation lifetime spectroscopy. Physica Status Solidi A, 2004, 201, 467-470.	1.7	22
273	The distribution of the unoccupied volume in glassy polymers. Journal of Molecular Graphics and Modelling, 2004, 22, 309-316.	2.4	28
274	Glass Transition Temperature in Thin Polymer Films Determined by Thermal Discharge in X-ray Photoelectron Spectroscopy. Macromolecules, 2004, 37, 8813-8815.	4.8	9
275	Investigation of the Surface Class Transition Temperature by Embedding of Noble Metal Nanoclusters into Monodisperse Polystyrenes. Macromolecules, 2004, 37, 1831-1838.	4.8	45
276	Dispersion of Gold in Polycarbonate by Vapor-Induced Crystallization. Macromolecules, 2004, 37, 2182-2185.	4.8	18
277	Tunable multiple plasmon resonance wavelengths response from multicomponent polymer-metal nanocomposite systems. Applied Physics Letters, 2004, 84, 2655-2657.	3.3	112
278	Polymer–metal optical nanocomposites with tunable particle plasmon resonance prepared by vapor phase co-deposition. Materials Letters, 2004, 58, 1530-1534.	2.6	78
279	Diffusion in metallic glasses and undercooled metallic melts. International Journal of Materials Research, 2004, 95, 956-960.	0.8	3
280	The effects of excimer laser irradiation on the surface morphology and self-adhesion properties of some engineering polymers as evaluated by ultrasonic welding. , 2004, , 193-252.		0
281	Production of gold nanoparticles-polymer composite by quite simple method. European Physical Journal D, 2003, 24, 365-367.	1.3	50
282	Investigation of the interaction of evaporated aluminum with vapor deposited Teflon AF films via X-ray photoelectron spectroscopy. Applied Physics A: Materials Science and Processing, 2003, 76, 851-856.	2.3	19
283	Silver diffusion in Fe40Ni38Mo4B18 metallic glass under high vacuum. Scripta Materialia, 2003, 48, 275-279.	5.2	2
284	Etching rate and structural modification of polymer films during low energy ion irradiation. Nuclear Instruments & Methods in Physics Research B, 2003, 208, 155-160.	1.4	33
285	Controlled growth of nano-size metal clusters on polymers by using VPD method. Surface Science, 2003, 532-535, 300-305.	1.9	53
286	Mechanisms of argon ion-beam surface modification of polystyrene. Surface Science, 2003, 532-535, 1040-1044.	1.9	33
287	Effects of thermal annealing of thin Au film on Fe40Ni38Mo4B18. Materials Science & Engineering A: Structural Materials: Properties, Microstructure and Processing, 2003, 351, 316-324.	5.6	5
288	Air oxidation of Zr65Cu17.5Ni10Al7.5 in its amorphous and supercooled liquid states, studied by thermogravimetric analysis. Physica Status Solidi A, 2003, 199, 431-438.	1.7	12

#	Article	IF	CITATIONS
289	Controlled Generation of Ni Nanoparticles in the Capping Layers of Teflon AF by Vapor-Phase Tandem Evaporation. Nano Letters, 2003, 3, 69-73.	9.1	72
290	Diffusion in metallic glasses and supercooled melts. Reviews of Modern Physics, 2003, 75, 237-280.	45.6	553
291	Diffusion and isotope effect in bulk-metallic glass-forming Pd–Cu–Ni–P alloys from the glass to the equilibrium melt. Journal of Materials Research, 2003, 18, 2688-2696.	2.6	26
292	Nanocomposites of Vapour Phase Deposited Teflon AF Containing Ni Clusters. Solid State Phenomena, 2003, 94, 285-294.	0.3	5
293	Diffusion in a Metallic Melt at the Critical Temperature of Mode Coupling Theory. Physical Review Letters, 2003, 90, 195502.	7.8	75
294	Diffusion Of Metals In Polymers And During Metal/Polymer Interface Formation. Springer Series in Advanced Microelectronics, 2003, , 221-251.	0.3	8
295	Evidence of diffusion via collective hopping in metallic supercooled liquids and glasses. Physical Review B, 2002, 65, .	3.2	30
296	Limits of Ion-Beam Depth-Profiling as Used in Diffusion Studies of Oxidation-Sensitive Materials. Defect and Diffusion Forum, 2002, 203-205, 147-152.	0.4	6
297	Free Volume Evolution in Bulk Metallic Glass during High Temperature Creep. Materials Research Society Symposia Proceedings, 2002, 754, 1.	0.1	0
298	Determination of the Binodal and Spinodal Phase Separation Temperatures in the Blend System PαMS0.5-co-AN0.5(Luran)/PMMA0.95MA0.05(Lucryl) with Positron Annihilation Lifetime Spectroscopy. Macromolecules, 2002, 35, 9074-9078.	4.8	13
299	Effect of composition and structure of gold/copper bimetallic nanoparticles on dispersion in polymer thin films. Journal of Materials Chemistry, 2002, 12, 3610-3614.	6.7	9
300	Evidence of noble metal diffusion in polymers at room temperature and its retardation by a chromium barrier. Applied Physics Letters, 2002, 81, 244-246.	3.3	43
301	Free Volume and Transport Properties in Highly Selective Polymer Membranes. Macromolecules, 2002, 35, 2071-2077.	4.8	239
302	Self-Assembled Nanowire Networks by Deposition of Copper onto Layered-Crystal Surfaces. Advanced Materials, 2002, 14, 1056.	21.0	36
303	Adsorption of Noble Metal Atoms on Polymers. , 2002, , 107-116.		3
304	Fundamental Aspects of Polymer Metallization. , 2002, , 73-96.		14
305	Embedding of Noble Metal Nanoclusters into Polymers as a Potential Probe of the Surface Glass Transition. Macromolecules, 2001, 34, 1125-1127.	4.8	87
306	Molecular Weight Dependence of the Surface Glass Transition of Polystyrene Films Investigated by the Embedding of Gold Nanoclusters. Materials Research Society Symposia Proceedings, 2001, 710, 1.	0.1	2

#	Article	IF	CITATIONS
307	Comparative Analysis of the Nucleation and Growth of Copper on Different Low-k Polymers. Materials Research Society Symposia Proceedings, 2001, 714, 811.	0.1	0
308	Does the diffusion mechanism in thin amorphous Co81Zr19films change during structural relaxation?. New Journal of Physics, 2001, 3, 6-6.	2.9	8
309	Study of oxidation behaviour of Zr-based bulk amorphous alloy Zr65Cu17.5Ni10Al7.5 by thermogravimetric analyser. Bulletin of Materials Science, 2001, 24, 281-283.	1.7	15
310	Surface oxidation of amorphous Zr65Cu17.5Ni10Al7.5 and Zr46.75Ti8.25Cu7.5Ni10Be27.5. Materials Science & Engineering A: Structural Materials: Properties, Microstructure and Processing, 2001, 304-306, 747-752.	5.6	48
311	Does the Diffusion Mechanism Change at the Caloric Glass Transition of Bulk Metallic Glasses?. Defect and Diffusion Forum, 2001, 194-199, 821-826.	0.4	6
312	Diffusion and Thermal Defects in Amorphous Metals. Defect and Diffusion Forum, 2001, 194-199, 833-840.	0.4	3
313	7Be tracer diffusion in a deeply supercooled Zr46.7Ti8.3Cu7.5Ni10Be27.5 melt. Applied Physics Letters, 2001, 79, 2892-2894.	3.3	16
314	X-ray reflectivity study on the surface and bulk glass transition of polystyrene. Physical Review E, 2001, 64, 061508.	2.1	49
315	Diffusion in Metallic Classes and Supercooled Melts. Materials Research Society Symposia Proceedings, 2000, 644, 211.	0.1	1
316	Condensation coefficients of noble metals on polymers: a novel method of determination by x-ray photoelectron spectroscopy. Surface and Interface Analysis, 2000, 30, 439-443.	1.8	28
317	Tailoring the Morphology of Metal/Polymer Interfaces. Advanced Engineering Materials, 2000, 2, 489-492.	3.5	26
318	Formation of metal–polymer interfaces by metal evaporation: influence of deposition parameters and defects. Microelectronic Engineering, 2000, 50, 465-471.	2.4	59
319	Isotope effect of Co diffusion in thin amorphous Co 51 Zr 49 layers during structural relaxation. Europhysics Letters, 2000, 51, 75-81.	2.0	13
320	Evidence of Highly Collective Co Diffusion in the Whole Stability Range of Co-Zr Glasses. Physical Review Letters, 2000, 84, 1467-1470.	7.8	35
321	Metal/polymer interfaces with designed morphologies. Journal of Adhesion Science and Technology, 2000, 14, 467-490.	2.6	97
322	Determination of condensation coefficients of metals on polymer surfaces. Surface Science, 2000, 454-456, 412-416.	1.9	15
323	Free Volume Distributions in Glassy Polymer Membranes:Â Comparison between Molecular Modeling and Experiments. Macromolecules, 2000, 33, 2242-2248.	4.8	102
324	On the Role of Thermal Defects in Diffusion in Metallic Glasses. Defect and Diffusion Forum, 1999, 165-166, 43-52.	0.4	4

#	Article	IF	CITATIONS
325	Interface structure and formation between gold and trimethylcyclohexane polycarbonate. Journal of Materials Research, 1999, 14, 3538-3543.	2.6	14
326	Condensation Coefficients of Ag on Polymers. Physical Review Letters, 1999, 82, 1903-1906.	7.8	78
327	Condensation coefficients and initial stages of growth for noble metals deposited onto chemically different polymer surfaces. Applied Surface Science, 1999, 144-145, 355-359.	6.1	65
328	Influence of thermal treatment on the morphology and adhesion of gold films on trimethylcyclohexane-polycarbonate. Applied Surface Science, 1999, 151, 119-128.	6.1	40
329	Correlation between fractional free volume and diffusivity of gas molecules in glassy polymers. Journal of Polymer Science, Part B: Polymer Physics, 1999, 37, 3344-3358.	2.1	174
330	Aluminum and silicon diffusion in Fe-Cr-Al alloys. Scripta Materialia, 1999, 40, 517-522.	5.2	24
331	Structural effects on diffusion in metallic glasses: The pressure dependence of Ni diffusion in as-quenched and relaxed Co42Zr58. Philosophical Magazine Letters, 1999, 79, 827-836.	1.2	13
332	Point defects and their properties in FeAl and FeSi alloys. Intermetallics, 1999, 7, 289-300.	3.9	58
333	Isotope effect of diffusion in the supercooled liquid state of bulk metallic glasses. Journal of Non-Crystalline Solids, 1999, 250-252, 684-688.	3.1	22
334	Positron-annihilation studies of free-volume changes in the bulk metallic glassZr65Al7.5Ni10Cu17.5during structural relaxation and at the glass transition. Physical Review B, 1999, 60, 9212-9215.	3.2	88
335	Nucleation, growth, interdiffusion, and adhesion of metal films on polymers. AIP Conference Proceedings, 1999, , .	0.4	8
336	Correlation between effective activation energy and pre-exponential factor for diffusion in bulk metallic glasses. Journal of Materials Research, 1999, 14, 3200-3203.	2.6	19
337	Correlation between fractional free volume and diffusivity of gas molecules in glassy polymers. Journal of Polymer Science, Part B: Polymer Physics, 1999, 37, 3344-3358.	2.1	116
338	Evidence of Aggregation-Induced Copper Immobilization During Polyimide Metallization. Advanced Materials, 1998, 10, 1357-1360.	21.0	30
339	Chemistry, diffusion and cluster formation at metal-polymer interfaces. Materials and Corrosion - Werkstoffe Und Korrosion, 1998, 49, 180-188.	1.5	43
340	Diffusion of metals in polymers. Materials Science and Engineering Reports, 1998, 22, 1-55.	31.8	233
341	Free-volume changes in the bulk metallic glassZr46.7Ti8.3Cu7.5Ni10Be27.5and the undercooled liquid. Physical Review B, 1998, 57, 10224-10227.	3.2	142
342	Evidence of Defect-Mediated Zirconium Self-Diffusion in AmorphousCo92Zr8. Physical Review Letters, 1998, 81, 614-617.	7.8	29

#	Article	IF	CITATIONS
343	Activation Volume ofC57oDiffusion in AmorphousCo81Zr19. Physical Review Letters, 1998, 80, 3288-3291.	7.8	50
344	Mass Dependence of Diffusion in a Supercooled Metallic Melt. Physical Review Letters, 1998, 80, 4919-4922.	7.8	113
345	Fundamental Aspects Of Polymer Metallization. Materials Research Society Symposia Proceedings, 1998, 511, 15.	0.1	12
346	Oxide Formation on the Bulk Metallic Glass Zr _{46.75} Ti _{8.25} Cu _{7.5} Ni ₁₀ Be _{27.5} . Materials Research Society Symposia Proceedings, 1998, 554, 167.	0.1	10
347	Free Volume Changes in Bulk Amorphous Alloys During Structural Relaxation and in the Supercooled Liquid State. Materials Research Society Symposia Proceedings, 1998, 554, 75.	0.1	1
348	Chemistry, diffusion and cluster formation at metal-polymer interfaces. Materials and Corrosion - Werkstoffe Und Korrosion, 1998, 49, 180-188.	1.5	1
349	Computer Simulation of Metal Diffusion in Polymers. Defect and Diffusion Forum, 1997, 143-147, 903-910.	0.4	14
350	Metal Diffusion in Polymers. Defect and Diffusion Forum, 1997, 143-147, 887-902.	0.4	24
351	Diffusion of Gold and Silver in Bisphenol A Polycarbonate. Macromolecules, 1997, 30, 567-573.	4.8	31
352	Diffusion of gold and silver in bisphenol trimethylcyclohexanen polycarbonate. Journal of Polymer Science, Part B: Polymer Physics, 1997, 35, 1043-1048.	2.1	22
353	Pressure and mass dependence of diffusion in metallic glasses. Journal of Non-Crystalline Solids, 1996, 205-207, 607-611.	3.1	7
354	The vanishing isotope effect of cobalt diffusion in Fe39Ni40B21glass. Journal of Physics Condensed Matter, 1995, 7, 7663-7668.	1.8	5
355	Absence of Isotope Effect of Diffusion in a Metallic Glass. Europhysics Letters, 1995, 29, 221-226.	2.0	30
356	Pressure dependence of cobalt diffusion in amorphous Fe39Ni40B21. Journal of Non-Crystalline Solids, 1995, 181, 261-265.	3.1	15
357	Highly Cooperative and Defect-Assisted Diffusion in Metallic Glasses. Defect and Diffusion Forum, 1993, 95-98, 1175-1180.	0.4	6
358	Positron Lifetime Spectroscopy in Polystyrene. Materials Science Forum, 1992, 105-110, 1613-1616.	0.3	6
359	An apparatus for ionâ€beam sputtering and its application to highâ€resolution radiotracer depth profiling of diffusion samples. Journal of Vacuum Science and Technology A: Vacuum, Surfaces and Films, 1992, 10, 92-97.	2.1	40
360	Pressure dependence ofCo60diffusion in amorphousCo76.7Fe2Nb14.3B7. Physical Review B, 1992, 45, 7459-7462.	3.2	25

#	Article	IF	CITATIONS
361	Isotope effect of Co diffusion in amorphousCo76.7Fe2Nb14.3B7. Physical Review B, 1992, 46, 120-125.	3.2	26
362	Feature article atomic transport: A review with perspectives. Philosophical Magazine A: Physics of Condensed Matter, Structure, Defects and Mechanical Properties, 1992, 65, 1287-1308.	0.6	6
363	Solute enhancement of silver self-diffusion in silver-tin alloys at low temperatures. Philosophical Magazine A: Physics of Condensed Matter, Structure, Defects and Mechanical Properties, 1992, 65, 207-214.	0.6	3
364	Transition from single-jump type to highly cooperative diffusion during structural relaxation of a metallic glass. Physical Review Letters, 1992, 68, 2347-2349.	7.8	69
365	Diffusion in Non-Crystalline Metallic and Organic Media. Physica Status Solidi A, 1992, 134, 9-59.	1.7	74
366	Pressure dependence of self-diffuson in FCC cobalt at low temperature. Scripta Metallurgica Et Materialia, 1991, 25, 2233-2238.	1.0	7
367	Chemistry, Microstructure, and Adhesion of Metal—Polymer Interfaces. , 1991, , 383-406.		13
368	Structural Investigation of the Silver—Polyimide Interface by Cross—Sectional Ten and Ion—Beam Sputtering. Materials Research Society Symposia Proceedings, 1990, 203, 59.	0.1	13
369	Metal diffusion in high-temperature polymers. Advanced Materials, 1990, 2, 266-268.	21.0	24
370	Pressure dependence and isotope effect of self-diffusion in a metallic glass. Physical Review Letters, 1990, 65, 1219-1222.	7.8	121
371	Stress development, intermetallic phase formation, and reaction kinetics in Coâ€Cr and Coâ€ī i thin films. Journal of Applied Physics, 1990, 67, 6807-6812.	2.5	1
372	Diffusion and Vacancy Impurity Interaction in Dilute fcc Alloys. Defect and Diffusion Forum, 1990, 66-69, 573-580.	0.4	1
373	Adhesion and deformation of metal/polyimide layered structures. Journal of Applied Physics, 1989, 65, 1911-1917.	2.5	66
374	Isochoric equilibrium studies of YBa 2 Cu 3 O x. Physica C: Superconductivity and Its Applications, 1989, 162-164, 905-906.	1.2	3
375	Direct measurements of Cu diffusion into a polyimide below the glass transition temperature. Applied Physics Letters, 1989, 55, 357-359.	3.3	55
376	Stress relaxation during thermal cycling in metal/polyimide layered films. Journal of Applied Physics, 1988, 64, 6690-6698.	2.5	54
377	Adhesion and deformation study of metal/polymer structures by a stretch deformation method. Applied Physics Letters, 1988, 53, 1602-1604.	3.3	46
378	Diffusion and vacancy-solute interaction in Ni-Si, Ni-Ge and Ni-Sn alloys. Journal of Physics F: Metal Physics, 1988, 18, 205-212.	1.6	14

#	Article	IF	CITATIONS
379	Excess Entropy in Vacancy-Impurity Binding. Materials Science Forum, 1987, 15-18, 1207-1212.	0.3	8
380	Equilibrium vacancies in Cu and Ag alloys with electropositive solutes. Philosophical Magazine A: Physics of Condensed Matter, Structure, Defects and Mechanical Properties, 1987, 56, 831-840.	0.6	10
381	Precision measurements of nonlinear solvent diffusion enhancement in α-Ag-As alloys. Acta Metallurgica, 1987, 35, 2273-2276.	2.1	7
382	The effect of non-random solute distribution around vacancies on the enhancement of solvent and solute diffusion. Acta Metallurgica, 1987, 35, 771-774.	2.1	18
383	Carbon-vacancy binding in Niî—,C alloys. Scripta Metallurgica, 1986, 20, 1755-1759.	1.2	24
384	Calculation of impurity-vacancy and impurity-impurity interactions from enhancement of solvent and solute diffusion. Physical Review B, 1986, 34, 2116-2124.	3.2	20
385	Calculation of the free enthalpy of impurity-vacancy binding from measurements of solvent diffusion. Scripta Metallurgica, 1984, 18, 597-599.	1.2	13
386	Solvent diffusion in α-silver-tin alloys. Acta Metallurgica, 1983, 31, 691-697.	2.1	33
387	Metal-polymer interfaces. , 0, , .		1
388	Encapsulating the active Layer of organic Thin-Film Transistors. , 0, , .		2
389	Characterization of Post Etch Residues Depending on Resist Removal Processes after Aluminum Etch. Solid State Phenomena, 0, 145-146, 349-352.	0.3	0
390	Influence of Metal Diffusion on the Electronic Properties of Pentacene and Diindenoperylene Thin Films. , 0, , 401-426.		0
391	Focus on Supersymmetry in Physics. New Journal of Physics, 0, 3, .	2.9	1